Annals of Nuclear Energy 37 (2010) 923–926

Contents lists available at ScienceDirect

Annals of Nuclear Energy

journal homepage: www.elsevier.com/locate/anucene

Indirect measurement of inelastic cross section of relativistic protons in Pb target

M. Zamani [a,*], S. Stoulos [a], M. Fragopoulou [a], M. Manolopoulou [a], M. Krivopustov [b]

[a] Aristotle University of Thessaloniki, School of Physics, Thessaloniki 54 124, Greece
[b] Joint Institute for Nuclear Research (JINR), Dubna 141980, Russia

ARTICLE INFO

Article history:
Received 5 February 2010
Received in revised form 29 March 2010
Accepted 31 March 2010

Keywords:
Spallation reactions
Inelastic proton cross section

ABSTRACT

The inelastic cross section of relativistic protons in Pb was determined indirectly by measuring the neutron distribution along a Lead spallation neutron source. The spallation neutron source was irradiated by 1, 1.5 and 2 GeV protons. The experimental results were obtained using passive methods. By the use of the beam attenuation coefficient, deduced by a fitting procedure of experimental data, the inelastic cross section of protons in Pb was determined.

1. Introduction

The spallation neutron sources proposed for the elimination of nuclear waste it is one of the most pressing issues during last decades. The spallation neutron sources are sub-critical neutron systems, driven by an accelerator (ADS). The accelerator bombards a target with high energy particles usually protons. Spallation reactions have been thoroughly investigated using energetic proton beams (Pienkowski et al., 1997; Hilscher et al., 1998; Lott et al., 1998; Carpenter, 1999 ; Letourneau et al., 2000). Another application of spallation reactions is related to the possibility of radioactive nuclei and production of exotic beams by neutron induced fission. Neutron beams are a fundamental tool in Solid State and Material Physics investigations, but also in applied research and industrial applications.

Spallation experiments have been also performed in Dubna using a large cylindrical Pb target surrounded by a paraffin moderator. In order to produce slow neutrons for transmutation purposes the moderator has been used to shift the hard spallation neutron spectrum to lower neutron energies (Wan et al., 2001; Adam et al., 2002; Westmeier et al., 2005). The prospect of building new facilities providing high intensity fast neutron beams for transmutation or incineration purposes via (*n,xn*) and (*n,f*) reactions has prompted to a renewal of interest in data related to spallation reactions induced by energetic light particles, such as protons or deuterons.

In order to perform transmutation experiments using a spallation neutron source, both calculation and measurements of produced neutron spectra by the spallation source are necessary. For the calculation of the produced neutrons, the inelastic cross section of the projectile particles with the target material must be known. Pb is one of the most common materials used in spallation sources. Several measurements have been made to estimate the inelastic cross section of protons with energies from few hundred MeV up to few GeV in Pb (Millburn et al., 1954; Chen et al., 1955; Goloskie and Strauch, 1962; Renberg et al., 1972; Letourneau et al., 2000; Dietrich et al., 2002; Amos et al., 2002; Auce et al., 2005; Herbach et al., 2006).

In the current work a measurement of the inelastic cross sections of 1, 1.5 and 2 GeV protons in Pb targets was performed. Neutron and proton distributions along the spallation source were performed using Solid State Nuclear Track Detectors (SSNTDs) and activation methods. The inelastic cross sections were determined from neutron and proton spatial distributions along the target applying a fitting procedure.

2. Experimental

The inelastic cross section of protons in Pb was determined by irradiation of a thick spallation target. The experimental set-up, "Gamma-2", consists of a cylindrical Pb target, with 40 cm length and 8 cm in diameter covered with a paraffin moderator 6 cm in thickness. The target irradiated by 1, 1.5 and 2 GeV proton beams, produce a fast neutron spectrum with a significant thermal-epithermal neutron component (Wan et al., 2001). The experiments have been performed at the Nuclotron accelerator, at High Energy Laboratory, JINR Dubna, Russia.

The neutron distribution was studied on the paraffin moderator along the target by using Solid State Nuclear Track Detectors (SSNTDs). CR39 foils acting as alpha particle detectors were placed parallel to the target axis. One part of the detectors was in contact

* Corresponding author. Tel./fax: +30 2310998176.
E-mail address: zamani@physics.auth.gr (M. Zamani).

0306-4549/$ - see front matter © 2010 Elsevier Ltd. All rights reserved.
doi:10.1016/j.anucene.2010.03.015

with a neutron converter, (Kodak LR115 type 2B, containing $Li_2B_4O_7$). The converter provides information about neutron fluence, detecting the alpha particles' tracks on CR39 emitted via $^{10}B(n,\alpha)^7Li$ and $^6Li(n,\alpha)^3H$ reactions. Another part of CR39 was in contact with the converter and was covered on both sides with 1 mm Cd foils detecting the epithermal and fast neutrons. The thermal neutron component (up to about 1 eV) was calculated by subtracting the measured track density of the Cd-covered from the Cd-uncovered region of the CR39 detector. Fast neutrons were also measured by proton recoil tracks on the detector itself (neutron elastic scattering on H of the detector) (Zamani and Savvidis, 1996). The neutron energy region detected by proton recoils is between 0.3 and 3 MeV due to the limitations in proton registration efficiency (Harvey et al., 1998).

Neutron distribution along the target at the paraffin surface was determined also by using activation detectors. Natural Cd foils (mass ~ 2 g, purity 99.9%, thickness 1 mm) were also used as an activation detector. The ^{nat}Cd effectively captures neutrons below 1 eV because of the high capture cross section of ^{113}Cd while it can be used for neutron detection above 1 eV via the $^{114}Cd(n,\gamma)^{115}Cd$ reaction (Manolopoulou et al., 2008). Moreover, ^{nat}Cd has a significant cross section to $^{nat}Cd(p,x)^{111}$. In reaction in the energy range of few MeV up to practically 400 MeV, responded well to the emitted proton spectrum (Bauer, 2001).

3. Results and discussion

Secondary neutrons and protons escape the paraffin surface covering the Pb target. The neutron spectrum contains a hard part corresponding to nuclear cascade effects taking place in the target. Theoretically, these high energy neutrons have energies up to the proton beam energy. Practically, secondary neutron energies reach about the half of the incident energy. Another neutron component superimposed on the fast neutron spectrum dominates the low energy part peaking at energies around 1 MeV. The low energy neutron spectrum can be attributed to light particle evaporation from the highly exited target nuclei during the intranuclear cascade reaction stage. However, what is observed at the moderator surface also includes a part of fast neutrons, shifted by the moderator, while high energy neutrons are slightly affected by the presence of the moderator. Therefore, along the paraffin surface and parallel to the target axis the beam attenuation can be observed by measuring neutron and proton fluencies.

Each part of the neutron spectrum was measured by using two different techniques as it is described in the experimental part of this work. In Fig. 1, neutron fluencies are presented for three neutron energy ranges. Thermal neutrons with $E_n < 1$ eV, slow (1 eV < E_n < 10 keV) and fast neutrons (0.3 MeV < E_n < 3 MeV) are shown for an irradiation of the target with protons of 1 GeV. Slow neutrons were measured by ^{nat}Cd activation method while thermal neutrons with $E_n < 1$ eV and fast neutrons by SSNTDs technique. Spatial distributions presented a similar behavior, peaked at about 10 cm from the target entrance. The ascendancy of fast neutrons against slow neutrons by one order of magnitude can be clearly deduced by Fig. 1.

Neutron fluence is depended on the proton beam energy hitting the target. It was measured by SSNTDs at the same positions for the proton energies of 1, 1.5 and 2 GeV and the results for fast neutrons are presented in Fig. 2. Experimental errors indicated are mainly due to the track measurement statistics and radiator response. Other parameters which contribute to the total experimental errors (i.e. radiator mass and beam intensity) can be considered of minor importance. The overall uncertainty for the specific measurements ranged between 17% and 21%. The spatial distribution has the same behavior for all energies, peaked at 10 cm downstream the target. Then a decrease is observed due to the beam attenuation. The same spatial distribution has been obtained during irradiations of the Pb target with 20 cm length irradiated by

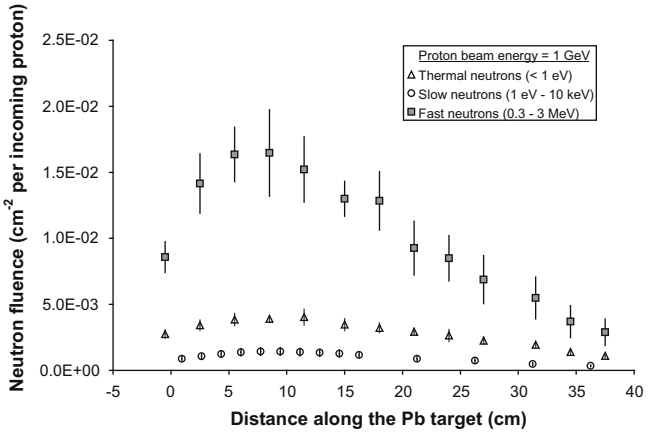

Fig. 1. Spatial neutron distribution along the target for various energy ranges obtained during irradiation by 1 GeV proton beam energy.

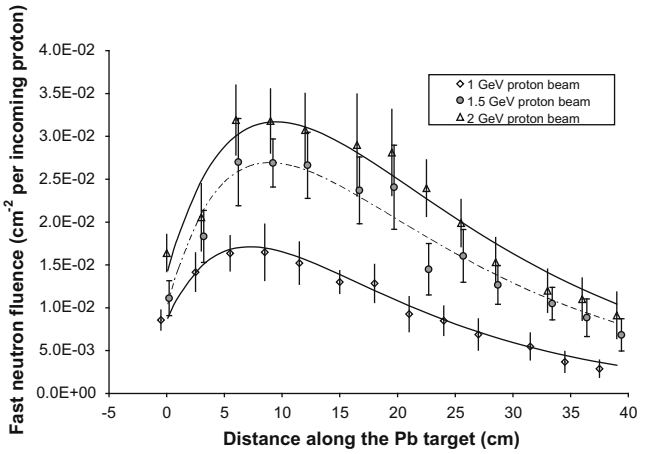

Fig. 2. Spatial neutron distributions along the target for various incoming proton beam energies. The lines referred to the fitting process using Eq. (1).

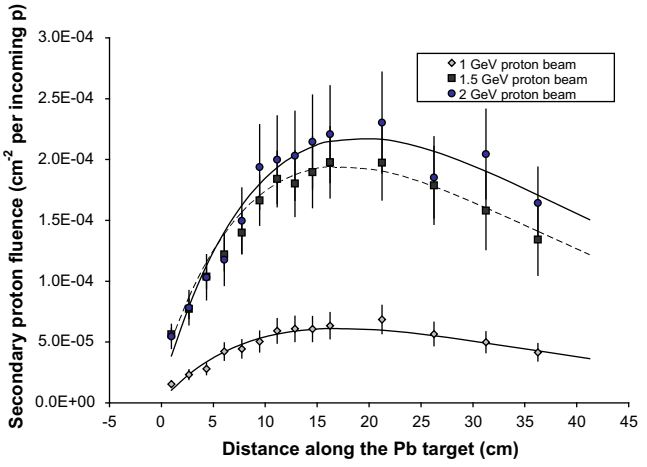

Fig. 3. Spatial proton distributions along the target for various incoming proton beam energies. The lines referred to the fitting process using Eq. (1).

Table 1
Fitting parameters on hadron spatial distributions using Eq. (1).

Fitting parameters	1 GeV proton beam		1.5 GeV proton beam		2 GeV proton beam	
	Fast neutron (SSNTDs)	Proton (Cd-activation)	Fast neutron (SSNTDs)	Proton (Cd-activation)	Fast neutron (SSNTDs)	Proton (Cd-activation)
Parameter C (cm^{-2} p^{-1})	0.050 ± 0.005	0.0024 ± 0.0006	0.066 ± 0.008	0.0103 ± 0.0062	0.099 ± 0.009	0.009 ± 0.005
Build-up parameter a	0.83 ± 0.03	1.00 ± 0.02	0.85 ± 0.03	1.00 ± 0.02	0.86 ± 0.02	1.00 ± 0.02
Build-up coefficient b (cm^{-1})	0.081 ± 0.004	0.0041 ± 0.0002	0.101 ± 0.006	0.0027 ± 0.0002	0.067 ± 0.006	0.0035 ± 0.0002
Attenuation coefficient d (cm^{-1})	0.069 ± 0.011	0.055 ± 0.007	0.053 ± 0.006	0.053 ± 0.005	0.056 ± 0.004	0.051 ± 0.006

protons with energy from 0.5 up to 7.4 GeV in previous experiments (Fragopoulou et al., 2006).

Protons generated by the target have energies high enough to pass through the moderator. Some of them are products of neutron interactions with the moderator materials. Their energies ranged between 10 and 100 MeV presented a peak around 50 MeV, as it was calculated by Monte Carlo code DCM-DEM (Manolopoulou et al., 2008). Spatial proton distributions measured by Cd activation are given in Fig. 3. For the energies studied in this experiment a similar behavior is observed, as shown in Fig. 3. The behavior is very close to that of neutrons and presents a maximum at 15–17 cm from the beam entrance in the target. The beam attenuation can be clearly deduced by the shape of the spatial distribution. Experimental errors indicated in Fig. 3 ranged between 15% and 22% and they are attributed mainly to effective cross section calculation and less to other sources as i.e. to the counting statistics, radiator mass and beam intensity.

The hadron fluencies per incident proton (ρ, cm^{-2} per incoming proton) were fitted by the consideration that two competitive effects take place inside the Pb target; an exponential increase of the secondary particle production at the head of the target, due to internuclear cascade (build up effect) and an exponential decrease of the proton beam intensity along the target (attenuation effect). The following equation was used (Bauer, 2001):

$$\rho = C(1 - ae^{-bx})e^{-dx} \quad (1)$$

where C is a parameter in units neutrons cm^{-2} $proton^{-1}$.

The first part of the equation was set to describe the build up effect with the build up parameter (a) and the build up coefficient (b, cm^{-1}). The second part represents the beam attenuation along the target as it was observed over the moderator surface with the attenuation coefficient (d, cm^{-1}). The attenuation coefficient d is related to the interaction length of primary protons in Pb. In fact, secondary particle production continues along the target but the energy of those particles is low, thus reducing further particle production. In a heavy target, protons and neutrons of low energies can induce fission reactions, which in case of a Pb target have very low cross section and can be neglected. Consequently, the decrease of neutron distribution along the target can be attributed mainly to the beam attenuation. Such considerations are valid for relatively large target dimensions compared to the range of protons hitting the heavy target, as in the case of Pb target used for the present study.

Using the attenuation coefficient d, the interaction length λ has been determined. The inelastic cross section of protons in Pb can be estimated by the relation between the interaction length and the inelastic cross section, $\sigma = A/N\lambda\rho$. A is the Pb atomic number, N is the Avogadro's number and ρ is the Pb target density (gr cm^{-3}) (Sullivan, 1992). By a similar fitting to proton experimental data, the inelastic cross sections of protons in Pb were also calculated. The values of the fitting parameters are presented in Table 1, for beam energies applied to those experiments. From the attenuation coefficient, d, given in Table 1 the inelastic cross sections have been calculated. One can observe that for all proton energies the inelastic cross sections are almost the same (Table 2) within the measurement uncertainties.

Table 2
Pb inelastic cross sections, in barns, for various incoming proton beam energies.

Proton energy (GeV)	Fast neutron (SSNTDs)	Proton (Cd-activation)	Mean value
1.0	2.09 ± 0.33	1.67 ± 0.21	1.79 ± 0.18
1.5	1.61 ± 0.18	1.61 ± 0.15	1.61 ± 0.12
2.0	1.70 ± 0.12	1.55 ± 0.18	1.65 ± 0.10

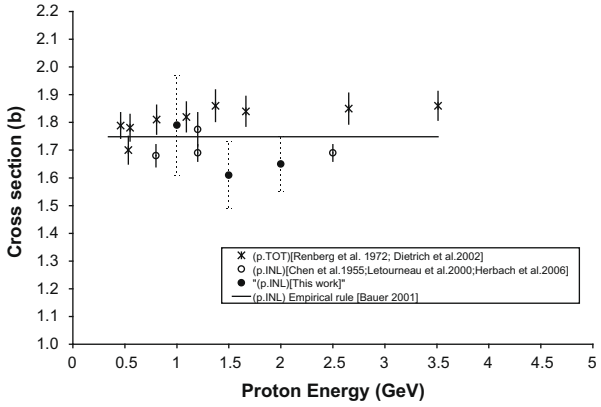

Fig. 4. Inelastic and total cross section data of relativistic proton induced reaction in Pb target.

It is interesting to note that inelastic cross sections can be equally determined by measuring the beam attenuation via neutrons or via protons at the paraffin surface. Independently of the particle-tracker used for the calculation of beam attenuation along the target, the inelastic cross sections are in good agreement with the inelastic cross sections of protons in Pb at the same energy region, as it is presented in literature (Chen et al., 1955; Renberg et al., 1972; Letourneau et al., 2000; Bauer, 2001; Dietrich et al., 2002; Herbach et al., 2006). In Fig. 4, a comparison of the experimental results of this work with data presented in literature are given. The line has been calculated by the relationship $\sigma_{inel} \sim 15\ \pi A^{2/3}$, given by Bauer (2001). The results coincide well to the literature data within experimental errors, about 10%. It has to be taken into account that the results of this work correspond to inelastic cross sections only, as they are deduced from measurements at large angles relative to the beam direction and therefore the elastic component is not included. The proton energy range is narrow for concluding results about the behavior of the cross section as a function of proton energy.

4. Conclusion

The use of protons in cross section experiments has the advantage of the possibility to have monoenergetic beams of well known energy and energy spread. Moreover it is in theory possible to determine the inelastic cross section accurately by absorbing out

the low energy secondaries. Protons, however, have several disadvantages resulting from the Coulomb field: the beam suffers ionization loss at the absorber. Also, at small angles, Rutherford scattering interferes with diffraction scattering making a determination of the total cross section exclusive of Coulomb scattering, very difficult except for elements of low *Z*. For these reasons, most of proton experiments have been designed to measure inelastic cross sections while most of neutron experiments to measure total cross sections.

From the above discussion is deduced that the experimental technique of the presented experiment can approach the inelastic cross section. Moreover the beam attenuation along the target has been followed at large emission angles where Rutherford scattering has practically no influence on cross section measurement. The determination was made by applying a fitting procedure to the experimental spatial hadron distribution along a Pb target measured on the paraffin moderator. For relativistic proton at energy range between 1 and 2 GeV the inelastic-total cross section in Pb is almost constant within the measurement uncertainty. The method can be also applied in other heavy targets, under the restriction that target dimensions are relatively small compared to the range of proton incident beam in the target.

Acknowledgments

The authors are grateful to Professor A.I. Malakhov and the staff of the Laboratory of High Energies, JINR Dubna, for their continuous support to our work. Special gratitude is due to Professor A.D. Kovalenko and the operation staff of the NUCLOTRON accelerator for providing high intensity beams during irradiations.

References

Adam, J. et al., 2002. Radiochim Acta. 90, 431.
Amos, K. et al., 2002. Phys. Rev. C65, 064618.
Auce, A. et al., 2005. Phys. Rev. C71, 064606.
Bauer, G.S., 2001. Nucl. Instrum. Methods Phys. Res. A 463, 505.
Carpenter, J.M., 1999. Physica B 270, 272.
Chen, F.F. et al., 1955. Phys. Rev. 99, 857.
Dietrich, F.S. et al., 2002. J. Nucl. Sci. Technol. 2, 269.
Fragopoulou, M. et al., 2006. Nucl. Instrum. Methods 560, 571.
Goloskie, R., Strauch, K., 1962. Nucl. Phys. A 92, 474.
Harvey, J.R. et al., 1998. Radiat. Prot. Dosim. 77, 267.
Herbach, C.M. et al., 2006. Nucl. Instrum. Method A 562, 729.
Hilscher, D. et al., 1998. Nucl. Instrum. Method Phys. Res. A 414, 100.
Letourneau, A. et al., 2000. Nucl. Instrum. Method Phys. Res. B 170, 299.
Lott, B. et al., 1998. Nucl. Instrum. Method Phys. Res. A 414, 117.
Manolopoulou, M. et al., 2008. Nucl. Instrum. Method Phys. Res. A 586, 239.
Millburn, G.P. et al., 1954. Phys. Rev 95, 1268.
Pienkowski, L. et al., 1997. Phys. Rev C 56, 1909.
Renberg, P.U. et al., 1972. Nucl. Phys. A 183, 81.
Sullivan, A.H., 1992. A Guide to Radiation and Radioactivity Levels near High Energy Particle Accelerators. Nuclear Technology Publishing, England.
Wan, J.S. et al., 2001. Nucl. Instum. Method Phys. Res. A 463, 634.
Westmeier, W. et al., 2005. Radiochim. Acta 93, 65.
Zamani, M., Savvidis, E., 1996. Radiat. Prot. Dosim. 63, 299.